Nuclear structure of ^{48}Ca

Y. Fujita
College of General Education, Osaka University, Toyonaka, Osaka 560, Japan

M. Fujiwara, S. Morinobu, T. Yamazaki, T. Itahashi, and H. Ikegami
Research Center for Nuclear Physics, Osaka University, Ibaraki, Osaka 567, Japan

S. I. Hayakawa
Ashikaga Institute of Technology, Ashikaga 326, Japan
(Received 30 March 1987)

The states of ^{48}Ca were studied by proton inelastic scattering at $E_p = 65$ MeV with an energy resolution of about 15 keV. The spectra obtained were highly structured and about 200 discrete levels were identified up to the excitation energy of 13.6 MeV. The widths of these levels were not noticeably wider than the instrumental energy resolution, even in the high excitation energy region above the neutron threshold. The values of transferred angular momentum L were assigned for most of the levels. The low-energy octupole resonance was observed as clustering $L=3$ states at the excitation energy between 7 and 12 MeV. In addition, many $L=2$ states and several $L=0$ states were observed above excitation energies of 10.5 and 12 MeV, respectively. These states are most likely the lower tails of giant quadrupole resonance and giant monopole resonance, respectively. Several unnatural parity states were clearly identified by comparing the (p,p′) spectra with (α,α') spectra obtained at a few angles. The spin and parity of each of these states were assigned with the aid of microscopic distorted wave analysis. Several states prominent at backward angles were identified to be high-spin stretched or nearly stretched states.

I. INTRODUCTION

Nuclei in the calcium region have always been attractive to test nuclear models and have been studied both experimentally and theoretically. Among the calcium isotopes, ^{40}Ca and ^{48}Ca are doubly magic nuclei. In particular, ^{48}Ca is the lightest doubly magic nucleus with neutron excess and published data indicate high purity of its doubly closed-shell structure.

Inelastic scattering on ^{48}Ca using (p,p′),[1–3] (p,p′γ),[4–7] and (α,α') reactions,[8,9] and also the (t,p) reaction[10] have given spectroscopic information on strongly populated states, especially in the low-lying region in ^{48}Ca. The ^{48}Ca(e,e′) reaction[11,12] has provided important information on unnatural parity states. These previous experimental data are summarized in the Nuclear Data Sheets.[13] Theoretical calculations of energy levels in ^{48}Ca have been performed by several authors.[14–17] These are all based on the shell model and one of them[14] uses the random-phase approximation (RPA) in the calculation process. Although ^{48}Ca is one of the best examples of a spherical nucleus because of its doubly closed-shell structure, little is known of the nuclear structure at high excitation energy, where various modes of nuclear excitation are expected.

One of the main subjects of this experiment is to search for collective modes of nuclear excitation at high excitation energy. Giant resonance (GR) is a fundamental mode which is related to a surface vibration of the nucleus.[18] The existence of electric GR has been experimentally established for the isoscalar monopole, isovector dipole, isoscalar quadrupole, and isoscalar octupole modes in heavier nuclei. These GR's have usually been observed as a broad bump. Recently, however, a high resolution (p,p′) study of the low-energy octupole resonance (LEOR) has revealed that the LEOR is composed of many discrete $L=3$ states and that the envelope of these states shows a resonancelike structure.[19] In the present (p,p′) experiment, the high resolution study is extended to the excitation region above the LEOR. It is our interest to examine whether or not other resonances will show up, and, if they do, what sort of features they have.

Unnatural parity states in ^{48}Ca are expected to have a simple structure because of the doubly closed-shell structure of ^{48}Ca. One of the states, the $J^\pi = 1^+$ state at $E_x = 10.2$ MeV is famous in relation to the discussion on quenching of the magnetic dipole strength. It is well known that comparing the (p,p′) spectra with (α,α') spectra is helpful in the identification of unnatural parity states. We decided to use this procedure in order to discover the candidates for unnatural parity states. Then, it is interesting to assign the J^π values for these states with the aid of microscopic distorted-wave calculations as well as with the aid of shell model calculations. The identification of high-spin stretched or nearly stretched states is also of interest.

In order to obtain accurate information on transferred angular momentum L (L transfer), we selected a fairly high proton incident energy of $E_p = 65$ MeV. Angular distributions of cross sections at this bombarding energy have more distinguishing features than those at lower

energies, yet they are not so forward-angle peaked as to make identification of small L transfers difficult. Since the levels are more closely spaced at higher excitation energies, a high resolution study with 15 keV resolution was performed in order to separate these states unambiguously, and to obtain accurate differential cross sections even for small peaks.

II. EXPERIMENTAL PROCEDURE

A proton beam from the RCNP cyclotron at Osaka University was used to bombard a ^{48}Ca self-supporting target foil with thickness and enrichment of 1.1 mg/cm^2 and 97.7%. Inelastically scattered protons were momentum analyzed by a magnetic spectrograph RAIDEN (Ref. 20) and detected with a 1.5 m long two-dimensional gas proportional counter.[21] Position information was obtained from this counter, while two ΔE counters and a plastic E counter placed behind the position counter enabled unambiguous identification of protons. One single measurement covered an energy range of about 3.5 MeV. Therefore, a complete spectrum up to $E_x = 14$ MeV was obtained by four measurements with different magnetic field settings for each angle. The angular distributions of protons were obtained for 14 angles between $\theta_{lab} = 8°$ and 70°. The acceptance angle was set at 3.2 msr and the kinematical line broadening in horizontal direction was compensated for by adjusting the field strengths of the elements of a multipole magnet at each angle.[22,23] The position and gate information was recorded on a magnetic tape event by event. Background counts due to slit scattering were largely subtracted by reanalyzing the data using the gate information. Finally, the overall resolution of 15 keV (full width at half maximum) was achieved by correcting the second-order kinematical effect in vertical direction.[21,23]

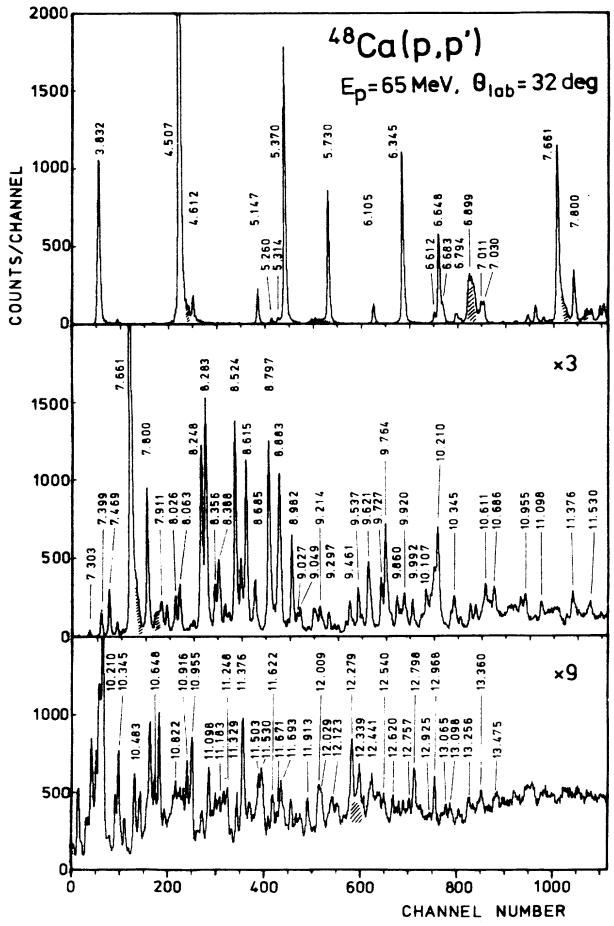

FIG. 1. Spectra of inelastically scattered protons on the ^{48}Ca target at $E_p = 65$ MeV. Prominent peaks are labeled with excitation energies in MeV. Peaks corresponding to contaminations are hatched.

Spectra at $\theta_{lab} = 32°$ is shown in Fig. 1. With a resolution of 15 keV, approximately 200 levels were observed. It should be noted that the widths of the levels in the spectra are not wider than the overall experimental energy resolution of 15 keV up to the excitation energy of 13.6 MeV. Absolute cross sections were obtained by calibrating both the target thickness and the whole detection system so as to get agreement between the measured cross sections of the proton elastic scattering and the results of the optical model calculation, described later. The absolute cross sections are believed to be accurate within 10%. The main uncertainty comes from the nonuniformity of the target thickness.

For the purpose of the parity assignment, the ^{48}Ca(α,α') experiment was performed at $E_\alpha = 70$ MeV with the same target. The spectra were taken at two angles of $\theta_{lab} = 13°$ and 16°. The former angle roughly corresponds to the expected local maxima of the angular distributions for the 1^- and 3^- states, while the latter angle to that for 2^+ states. Measurements at the two angles were also important for discriminating against contaminant peaks.

III. DATA ANALYSIS

A. Excitation energy

The excitation energy was carefully determined for every state observed in the (p,p') spectra. The energies of the low-lying levels in ^{48}Ca have been determined with high precision by high resolution (p,p') and γ-ray measurements.[13] In the present analysis, prominent low-lying states with well-known excitation energies (denoted by an asterisk in Table I) were used as standards in the energy calibration. First, the magnetic field of the spectrograph was varied for these peaks of interest to appear at various points on the focal plane. By using the obtained peak positions, the magnetic fields, and results of kinematical calculation, the mean radii of the proton flight orbits were determined at various points on the focal plane. These points were interpolated by a smooth curve and the mean radius R was determined as a function of the peak position x on the focal plane. Then the magnetic rigidity $B\rho$ of a particle which hits the position x can be determined by using the field strength B of the spectrograph as

$$B\rho = BR(x)g(B)\ , \tag{1}$$

where $g(B)$ has a value of almost unity and varies slowly as a function of B. The correction factor $g(B)$ is important in the accurate determination of excitation energy.[24] The incident proton energy was also carefully estimated. Finally, the excitation energies of unknown levels were determined with the help of kinematical calculations. The overall accuracy was estimated to be ± 7 keV for the levels with $E_x \leq 8$ MeV. The error was mainly due to uncertainties in the energy loss in the target, beam energy, and determination of peak centroid. For excitation energies above 8 MeV, an additional 1 keV error for every 1 MeV increase in excitation energy should be added to ± 7 keV.

The excitation energies of all the observed states are tabulated in Table I. For comparison, the results from the previously published data on ^{48}Ca are also given. They include the ^{48}Ca(p,p') data at 25–40 MeV,[1] at 160 MeV,[3] and (e,e') data.[12]

The impurity in the target was mainly ^{40}Ca (2.2%). At a few angles, reference (p,p') spectra from a ^{40}Ca target were measured under the same condition as for the ^{48}Ca target. As a result only several strongly excited levels in ^{40}Ca (Ref. 25) could be identified in ^{48}Ca spectra. These levels were identified also by the shift of peak position with angle due to the kinematical effect. All the levels corresponding to contaminations of light elements such as ^{1}H, ^{12}C, ^{13}C, and ^{16}O could be identified by their broad peak widths and by their larger angular energy shifts due to the kinematical effect. Some of the contaminant peaks prominent in the spectrum are hatched in Fig. 1.

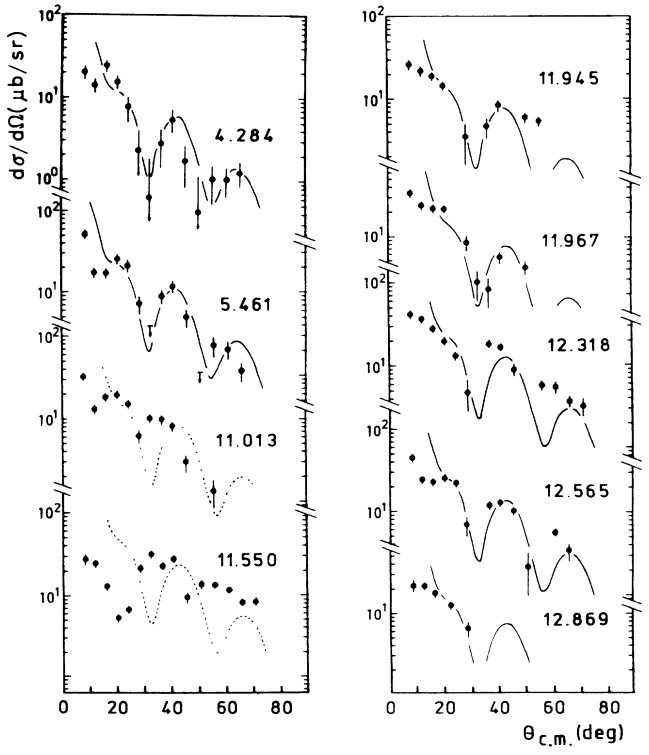

FIG. 2. Experimental $L=0$ angular distributions observed in the ^{48}Ca(p,p') reaction. The lines represent $L=0$ DWBA calculations.

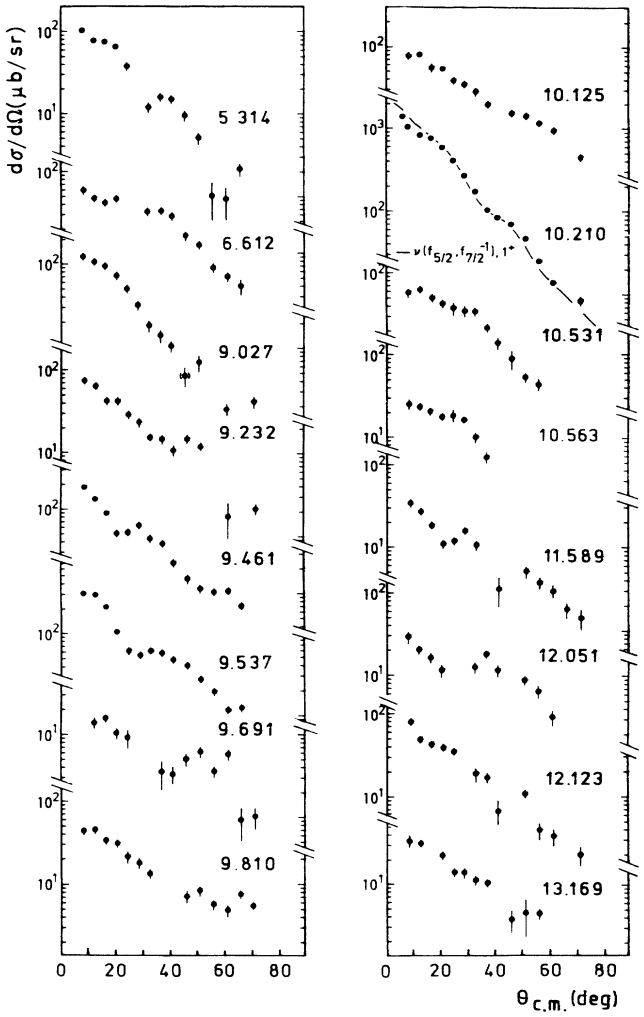

FIG. 3. Experimental $L=1$ angular distributions. The $J^\pi = 1^+$ state at $E_x = 10.210$ MeV is included for comparison. The solid line for this state represents a microscopic DWBA calculation for the $\nu(f_{5/2}, f_{7/2}^{-1})$, $J^\pi = 1^+$ state.

B. Assignment of L values

The spectra of ^{48}Ca were analyzed at angles from $\theta_{lab} = 8°$ to 70° up to $E_x = 13.6$ MeV. In order to obtain accurate cross sections for individual levels, a peak deconvolution program,[26] which uses the well-separated low-lying levels as peak shape standards, was utilized in the analysis. The angular distributions for most of the resolved levels are shown in Figs. 2–8. The errors shown in the figures are the square roots of the quadratic sum of the statistical error and the error from peak deconvolution.

The distorted-wave Born-approximation (DWBA) calculation was performed with the code DWUCK (Ref. 27) using a collective-model form factor. For the calculation

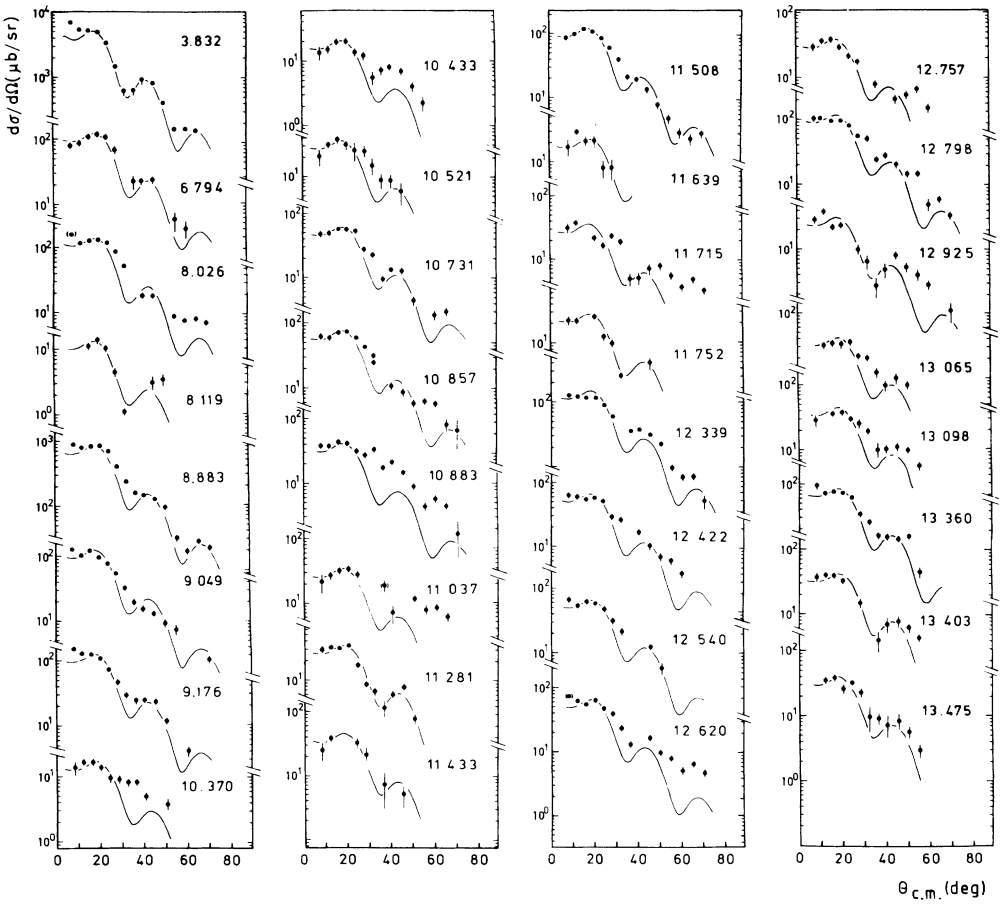

FIG. 4. Experimental $L=2$ angular distributions. The solid lines represent $L=2$ DWBA calculations.

of 0^+ states, a modified version of DWUCK (Ref. 28) and a form factor of Satchler's version I (Ref. 29) was used. The optical potential parameters were taken from a systematic study of Sakaguchi *et al.*,[30] and are given in Table II.

The transferred angular momentum L was assigned by comparing the experimental angular distribution either with theoretical angular distributions, or with the experimental angular distributions for states with established spin and parity. The calculations compared to the data points are shown by solid lines in Figs. 2–8. The $J^\pi=1^+$ state at $E_x=10.210$ MeV is included in the figure of $L=1$ (Fig. 3) for comparison. The results are tabulated in column 2 of Table I. Values given in parentheses indicate tentative assignments. These tentative values are unlikely to be in error by more than one unit. Several peaks were found to have angular distributions which were well described as two overlapping states with small and large L transfers. These levels, and the states which are fitted well with $L\geq 6$, are summarized in Fig. 8.

In order to distinguish natural parity states from unnatural parity states, one to one correspondence between a level observed in the (p,p′) reaction and a level in the (α,α') spectra was checked up to the excitation energy of 12 MeV. Although the resolution of (α,α') spectra (see Fig. 1 of Ref. 31) was worse ($\sim$30 keV) than that of (p,p′) spectra ($\sim$15 keV), most of the peaks in (α,α') spectra were consistently identified by referring to the levels observed in the (p,p′) reaction. In order to show the certainty in observation and identification, levels observed in the (α,α') reaction at $\theta_{\rm lab}=13°$ and/or 16° were classified into the following three categories:

(A) clearly observed;
(B) weak, or less clear, but certainly observed;
(C) likely, but not clearly observed.

These classifications are shown in column 3 of Table I. States which were not observed or not identified in (α,α') spectra are not categorized. As a result of these classification, identified spins and parities are shown in column 4 of Table I.

The deformation length $\beta_L R$ was obtained by comparing the data with the results of the DWBA calculation, namely

$$(\beta_L R)^2_{\rm expt}=[(d\sigma/d\Omega)_{\rm expt}/(d\sigma/d\Omega)_{\rm DWBA}]R^2\ . \qquad (2)$$

The fraction S of the energy weighted sum rule (EWSR) for an isoscalar state was then derived by using a procedure given in the literature.[32] A state of multipolarity L ($L\geq 2$) located at E_x which completely exhausts the EWSR has a deformation length

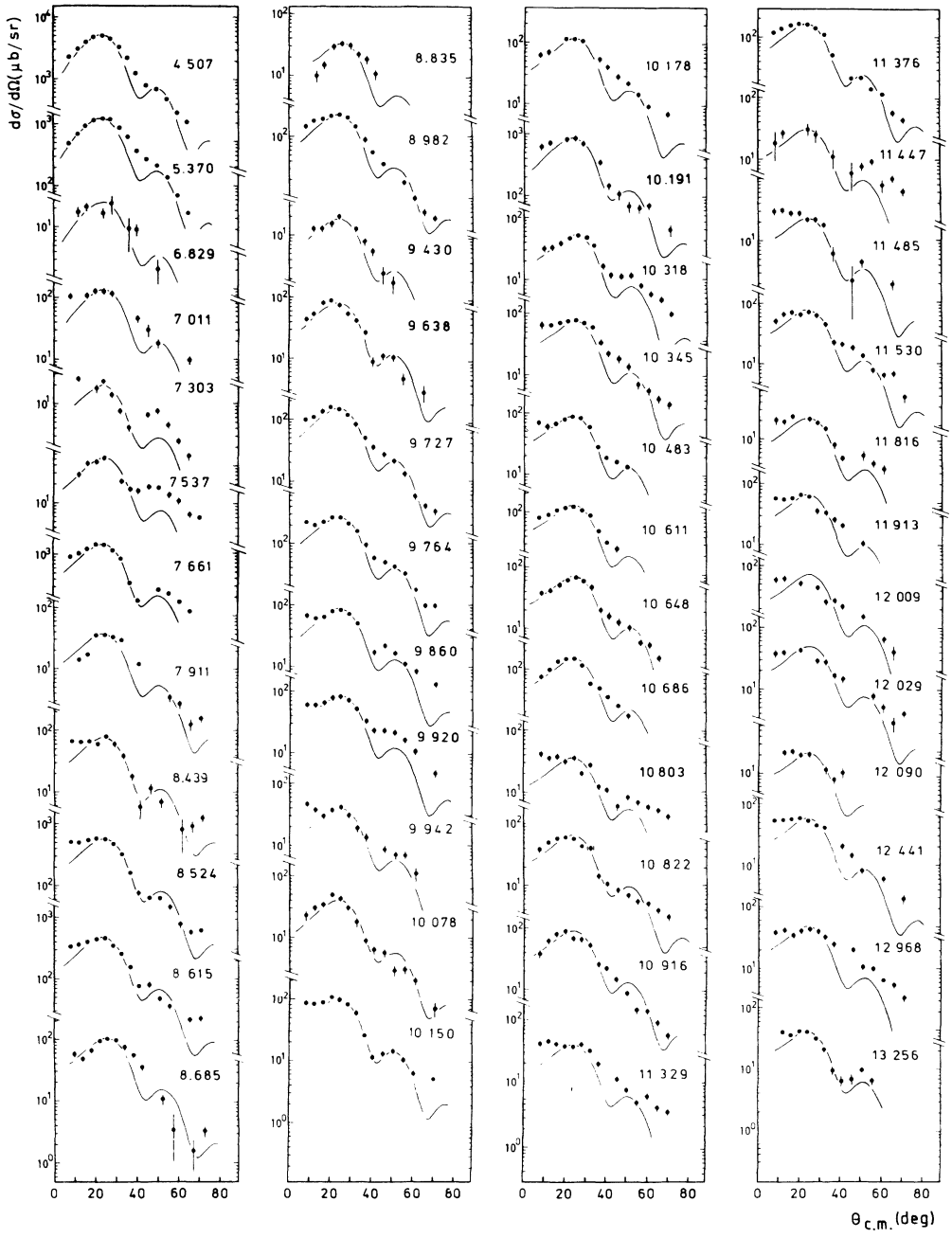

FIG. 5. Experimental $L=3$ angular distributions

$$(\beta_L R)^2=(4\pi/3A)(\hbar^2/2ME_x)L(2L+1)\ , \tag{3}$$

where A is the mass number and M is the nucleon mass. Similarly, for the monopole excitations[29]

$$(\beta_0 R)^2=20\pi\hbar^2/6MAE_x\ . \tag{4}$$

Then the S value is obtained from

$$S=(\beta_L R)^2_{\text{expt}}/(\beta_L R)^2\ . \tag{5}$$

The strengths obtained assuming isoscalar natural parity states are given in Table I in the form of deformation length $(\beta_L R)$ and EWSR fraction (S), where the radius R of $r_0 A^{1/3}$ was used.

The strength distributions for the states of $L=0$, 2, 3, 4, 5, and 6 are shown in Fig. 9 as fractions of the EWSR. Here, the strength distributions for $L=2$ and 3 states given in the previous paper[19] are slightly modified, because some of the states have been clearly identified not to be natural parity states by the procedure described above.

C. Continuum background

As seen from Fig. 1, background counts gradually increase above $E_x=10$ MeV. This value of 10 MeV corre-

TABLE I. Summary of the present results and comparison with previous works. The values in parentheses are less certain. The energy value used for the energy calibration is denoted by an asterisk.

Present work						40 MeV (p,p')[a]			160 MeV (p,p')[b]		(e,e')[c]	
E_x (MeV)	L	Category	J^π	βR (fm)	S (%)	E_x (MeV)	L	βR	E_x (MeV)	J^π	E_x (MeV)	J^π
3.832*	2	A	2^+	0.61	7.82	3.830	2	0.70	3.832	2^+	3.837	2^+
4.284	0	B	0^+	0.05	0.13							
4.507*	3	A	3^-	0.76	6.85	4.505	3	0.81	4.507	3^-	4.507	3^-
4.612*			(3^+)			4.608	4	0.22	4.613		4.608	3^+
5.147*	5	A	5^-	0.16	0.14	5.146	5	0.22	5.147	4	5.147	5^+
5.260			(5^+)			5.252	5	0.11			5.252	(4^-)
5.314	1	C	(1^-)			5.304						
5.370*	3	A	3^-	0.38	2.04	5.368	3	0.46	5.368	3^-	5.372	3^-
5.461*	0	B	0^+	0.08	0.34							
5.730	5	A	5^-	0.37	0.79	5.729	5	0.46	5.729	(5^-)	5.726	5^-
6.105		C	(4^-)			6.104	5	0.15	6.104	4	6.105	4^-
6.345	4	A	4^+	0.32	1.00	6.342	4	0.37	6.342	4^+	6.340	4^+
6.612	(1)	B	(1^-)									
6.648	4	A	4^+	0.24	0.60	6.648	4	0.25	6.648	4^+	6.647	4^+
6.683	1,2		2^-								6.689	(2^-)
									6.755	<3		
6.794	2	A	2^+	0.10	0.35	6.795					6.796	$(1^-,2^+)$
6.829	(3)			0.05	0.05							
6.899	(2)[d]	C		0.05	0.10						6.893	$(5^+,2^-)$
	+ (5)[d]			0.08	0.04	6.897	5	0.15	6.897	$\gtrsim 3$		
7.011	3	B	3^-	0.13	0.30				7.009	<3		
						7.019					7.018	$(5^-,3^-,6^+)$
7.030	3	C		0.06	0.07							
	+ 6			0.13	0.08							
7.303	3	B	3^-	0.05	0.05	7.298					7.286	(1^-)
7.399	1,2	C	(2^-)			7.401	3	0.15			7.397	(4^-)
7.442												
7.469	4	A	4^+	0.11	0.13	7.468					7.476	(4^+)
7.494									7.500	3		
7.537	3	A	3^-	0.08	0.12	7.536						
7.575												
7.661	3	A	3^-	0.41	3.34	7.659	3	0.49	7.659		7.657	3^-
7.800	4	A	4^+	0.19	0.41	7.801	4	0.22	7.800	4^+	7.791	(4^+)
7.911	3	A	3^-	0.06	0.09							
7.956	4	C	(4^+)	0.08	0.08						7.953	$(2^-,6^-)$
8.001		B										
8.026	2	B	2^+	0.10	0.48						8.038	$(1^-,2^+)$
						8.047			8.047	<2		
8.063	5	A	5^-	0.14	0.16							
8.119	2			0.04	0.06						8.113	
8.178	4	A	4^+	0.05	0.03							
8.236	5			0.12	0.12							
8.248	4	B	4^+	0.21	0.58							
						8.269	4	0.22	8.269	4^+		
8.283	4	A	4^+	0.25	0.79						8.272	$(4^+,5^-)$
8.356	5	A	5^-	0.13	0.15							
8.388	1	A	1^-									
	+ 6		(6^+)	0.16	0.16	8.385	5	0.25	8.385		8.385	(3^-)
8.439	3	A	3^-	0.10	0.21						8.435	
8.471	4			0.07	0.07						8.477	
8.524	3	A	3^-	0.27	1.58	8.522	3	0.26			8.518	3^-
8.570	(6)[d]		$(6^+,6^-)$	0.22	0.30	8.562	5	0.27	8.572	3	8.557	6^-
8.615	3	A	3^-	0.24	1.27	8.608	3	0.27	8.609	3^-	8.605	3^-
8.685			(3^+)			8.680	3	0.07				
8.698		C										
8.788												
8.797	4	A	4^+	0.21	0.60							
	+ 6		(6^+)	0.30	0.55	8.806	5	0.41	8.811		8.804	5^-

TABLE I. (*Continued*).

	Present work					40 MeV (p,p')[a]			160 MeV (p,p')[b]		(e,e')[c]	
E_x (MeV)	L	Category	J^π	βR (fm)	S (%)	E_x (MeV)	L	βR	E_x (MeV)	J^π	E_x (MeV)	J^π
8.835	3			0.06	0.10							
8.866	5	C	(5^-)	0.16	0.23							
8.883	2	A	2^+	0.25	3.10	8.885	5	0.30	8.885	2	8.884	$(1^-,2^+)$
8.918												
8.947												
8.982	3	A	3^-	0.17	0.65							
9.027	1	B	1^-						9.010	<4		
											9.038	
9.049	2	B	2^+	0.10	0.48							
9.079												
9.117	2			0.05	0.12							
	+ (8)[d]		(7^-)								9.138	8^-
9.158	4	C	(4^+)	0.08	0.08				9.150	>4		
9.176	2	B	2^+	0.10	0.46							
9.214	3	C	(3^-)	0.07	0.14							
	+ (7)[d]		$(6^-,7^-)$						9.229	$8^+,8^-$		
9.232	(1)											
											9.276	8^-
9.297	1	A	1^-								9.290	2^+
	+ (8)[d]		(8^-)						9.307	$8^+,8^-$		
9.334												
9.367	6			0.09	0.05							
9.430	3			0.05	0.06							
9.461	1	A	1^-									
9.496												
9.537	1	A	1^-									
											9.550	3^-
9.568	(6)			0.10	0.06							
9.621	4	A	4^+	0.13	0.27							
9.638	3			0.10	0.26							
9.691	(1)											
9.727	3			0.14	0.49							
9.764	3	A	3^-	0.18	0.85							
9.784	(4)			0.07	0.08							
9.810	1	C	(1^-)									
9.860	3	B	3^-	0.10	0.28							
9.893	3			0.06	0.08							
	+ (6)			0.08	0.04							
9.920	3	B	3^-	0.10	0.27							
9.942	3			0.07	0.13							
											9.953	8^-
9.992	4	B	4^+	0.09	0.13							
10.065	4	C	(4^+)	0.07	0.07							
10.078	3	C	(3^-)	0.07	0.14							
10.107	4	B	4^+	0.12	0.21							
10.125	1	B	1^-									
10.150	3	B	3^-	0.11	0.34							
10.178	3	A	3^-	0.12	0.40							
10.191	3	B	3^-	0.10	0.27							
10.210	1		1^+						10.22	1^+		
10.265												
10.318	3	B	3^-	0.08	0.18							
10.345	3	B	3^-	0.11	0.31							
10.370	2	C	(2^+)	0.04	0.08							
10.399	4			0.07	0.07							
10.433	2			0.04	0.09							
10.483	3	A	3^-	0.11	0.31							
10.521	2	C	(2^+)	0.05	0.17							
10.531	(1)	C										

TABLE I. (*Continued*).

	Present work					40 MeV (p,p')[a]			160 MeV (p,p')[b]		(e,e')[c]	
E_x (MeV)	L	Category	J^π	βR (fm)	S (%)	E_x (MeV)	L	βR	E_x (MeV)	J^π	E_x (MeV)	J^π
10.563	1,2											
10.586	4	C	(4^+)	0.08	0.09							
10.611	3	A	3^-	0.13	0.47							
10.623												
10.648	3	C	(3^-)	0.10	0.26							
10.686	3	A	3^-	0.14	0.54							
10.731	2	B	2^+	0.07	0.29							
10.745												
10.765												
10.782												
10.803	(3)	C	(3^-)	0.07	0.13							
10.822	3	B	3^-	0.09	0.24							
10.857	2	A	2^+	0.08	0.35							
10.872	6			0.09	0.07							
10.883	(2)	A	(2^+)	0.06	0.21							
10.916	3	C	(3^-)	0.11	0.33							
10.936												
10.955	4	A	4^+	0.12	0.26							
11.013												
11.037	(2)	C	(2^+)	0.05	0.18							
11.050	(4)			0.07	0.09							
11.098	2	A	2^+	0.07	0.32							
	+4		4^+	0.09	0.14							
11.125	4			0.06	0.05							
11.153												
11.183	(5)	C	(5^-)	0.09	0.09							
11.219		C										
11.230												
11.248	4	C	(4^+)	0.09	0.14							
11.281	2	B	2^+	0.05	0.17							
11.329	3	B	3^-	0.07	0.15							
11.376	3	A	3^-	0.14	0.63							
11.421												
11.433	2			0.06	0.24							
11.447	3			0.06	0.11							
11.466												
11.485	(3)			0.05	0.09							
11.508	2	A	2^+	0.10	0.61							
11.530	3	A	3^-	0.10	0.31							
11.550		C										
11.589	1											
11.622	(4)	B	(4^+)	0.09	0.13							
11.639	(2)			0.04	0.12							
11.671	(5)			0.06	0.04							
	+(8,9)[d]		(8^-)									
11.693	5	A	5^-	0.11	0.14							
11.715	(2)			0.05	0.19							
11.752	2	C	(2^+)	0.05	0.15							
11.773		C										
11.816	3			0.05	0.09							
11.828												
11.848		C										
11.913	3	A	3^-	0.09	0.27							
11.945	0		(0^+)	0.07	0.58							
11.967	0		(0^+)	0.07	0.56							
12.009	(3)	B	(3^-)	0.10	0.30							
12.029	3	B	3^-	0.08	0.21							
12.051	(1)											
12.090	(3)			0.05	0.09							
12.107	5			0.08	0.08							

TABLE I. (*Continued*).

	Present work				40 MeV (p,p')[a]			160 MeV (p,p')[b]		(e,e')[c]	
E_x (MeV)	L	Category	J^π	βR (fm)	S (%)	E_x (MeV)	L	βR	E_x (MeV)	J^π	E_x (MeV)	J^π
12.123	1											
12.162	4			0.08	0.12							
12.176												
12.216	5			0.05	0.04							
12.271	(4)			0.10	0.20							
12.318	0		(0^+)	0.09	1.10							
12.339	2			0.11	0.85							
12.369	(4)			0.06	0.07							
12.422	2			0.07	0.38							
12.441	3			0.09	0.25							
12.476												
12.499												
12.540	2			0.07	0.36							
12.565	0		(0^+)	0.09	1.03							
12.620	2			0.07	0.38							
12.658												
12.667												
12.704												
12.757	2			0.06	0.22							
12.798	2			0.10	0.68							
12.846												
12.869	(0)			0.06	0.54							
12.925	2			0.05	0.18							
12.968	(3)			0.08	0.22							
13.030	5			0.07	0.06							
13.065	(2)			0.06	0.25							
13.098	2			0.06	0.27							
13.169	1											
13.223												
13.256	3			0.08	0.20							
13.290												
13.360	2			0.09	0.54							
13.403	2			0.06	0.26							
13.439												
13.475	2			0.06	0.25							
13.493												

[a]Reference 1.
[b]Reference 3.
[c]Reference 12.
[d]See text.

sponds to the neutron separation energy ($S_n = 9.944$ MeV), where the continuum from the (p,pn) reaction should begin. This fact suggests that the amount of other background is small. The angular distributions were derived for the background counts in the $E_x = 10.7$, 12.3, and 13.2 MeV regions, respectively, and are shown in Fig. 10, where the cross section per 100 keV is plotted. The angular distributions for $\theta < 30°$ are rather flat, while at larger angles, the cross sections gradually decrease.

IV. DISCUSSION AND ANALYSIS

A. Low-lying states

The level scheme of ^{48}Ca in the highly excited region has not been well established. Even in the low-excitation region, the identification of some states was still under discussion. For several states, however, it appears possible that significant limitations can be placed on the spins and the parities by comparing the (p,p') spectra with those of the (α,α') reaction. Here we discuss some selected low-lying states by comparing the present results with those of previous works.

1. 3.832, 4.507, 5.370, 6.345, and 6.648 MeV states

These low-lying states are strongly excited in both (p,p') and (α,α') reactions. The J^π values proposed are 2^+, 3^-, 3^-, 4^+, and 4^+, respectively, and these assignments and obtained strengths are in good agreement with those of previous work as listed in Table I.

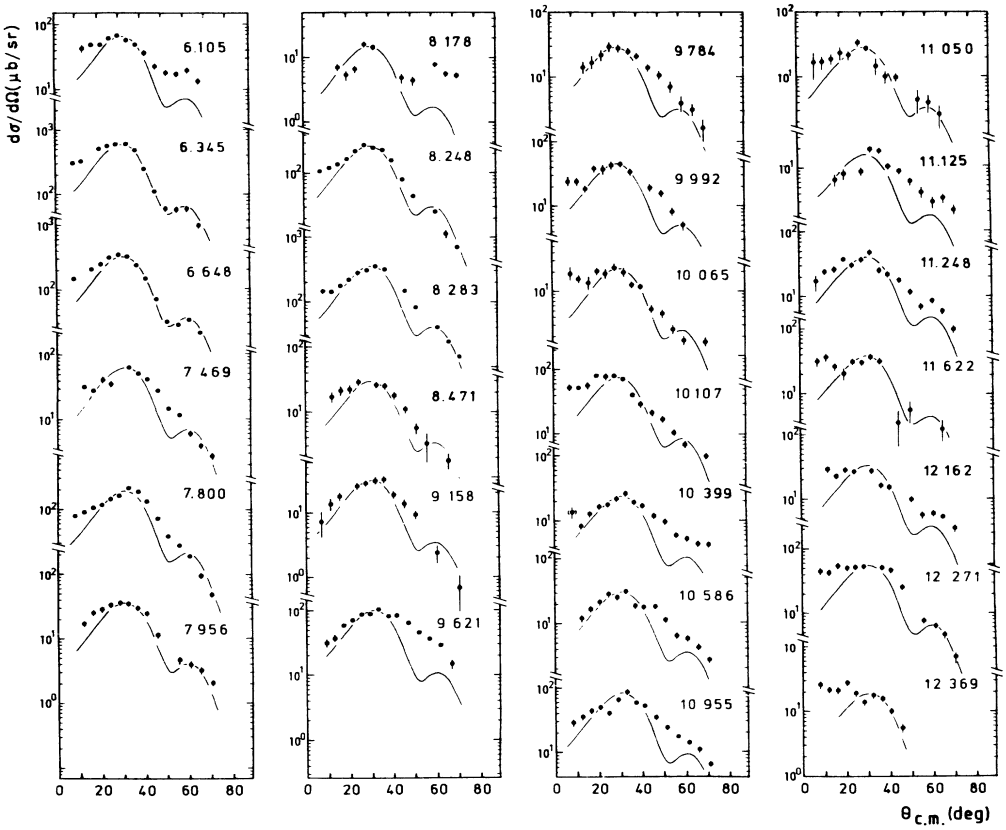

FIG. 6. Experimental $L=4$ angular distributions

A ^{48}K β-decay experiment[33] and a (p,p'γ) experiment[6] suggest that there is a 4.503 MeV, $J^{\pi}=4^{+}$ state. This state was not resolved from the first 3^{-} state at 4.507 MeV in our experiment. However, the contribution of the 4.503 MeV state to the cross section of the 4.507 MeV 3^{-} state seems to be small, because the second 3^{-} state at 5.370 MeV shows an angular distribution quite similar to the 4.507 MeV state.

2. 5.147, 5.260, and 5.730 MeV states

The first maximum in the angular distribution of these states coincides with the $L=5$ DWBA prediction in the (p,p') reaction. Among them, 5.147 and 5.730 MeV states were both clearly observed in the (α,α') spectra and the intensity ratio of the two states was nearly the same as that of the (p,p') reaction. All the previous works have assigned $J^{\pi}=5^{-}$ for the 5.730 MeV state, but the assignment for the 5.147 MeV state has been rather ambiguous. The (p,p'γ) coincidence experiments[4,6] restrict the spin to 5. A (p,p') study of $E_p=25$–40 MeV (Ref. 1) suggests $L=5$, but in a (p,p') reaction at $E_p=160$ MeV,[3] $L=4$ is favored. An (e,e') experiment[12] suggests 5^{+}. An unnatural parity assignment is excluded by the clear observation of this state in the (α,α') spectra. We suggest $J^{\pi}=5^{-}$ for this state.

The 5.260 MeV state was not observed in the spectra of the (α,α') reaction, which suggests that this state is an unnatural parity state. More detailed discussion will be given later.

3. Low-lying 0^{+} states

The 4.284 and 5.461 MeV states have been clearly identified to be $J^{\pi}=0^{+}$ by a ^{46}Ca (t,p)^{48}Ca reaction[10] and

TABLE II. Optical-model parameters used in the DWBA calculations. The form of the potential is the same as that given in Ref. 30. The Coulomb radius r_C is 1.25 fm.

	(MeV)		(fm)		(fm)
V	32.907	r_0	1.230	a_0	0.6808
W	10.228	r_W	1.187	a_W	0.7824
W_D	2.515	r_D	1.344	a_D	0.3975
V_{so}	5.680	r_{so}	1.091	a_{so}	0.6475

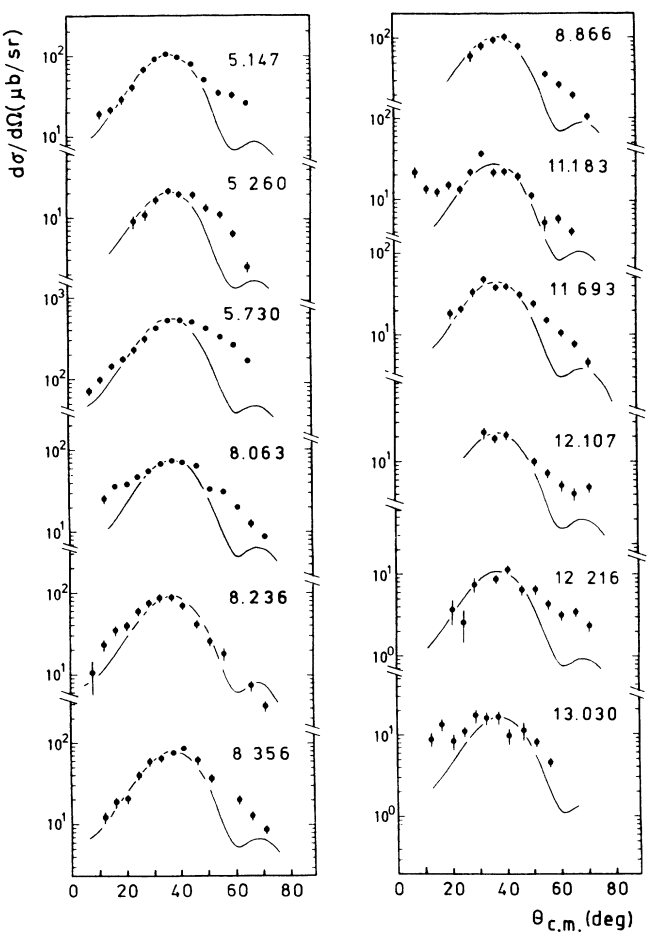

FIG. 7. Experimental $L=5$ angular distributions

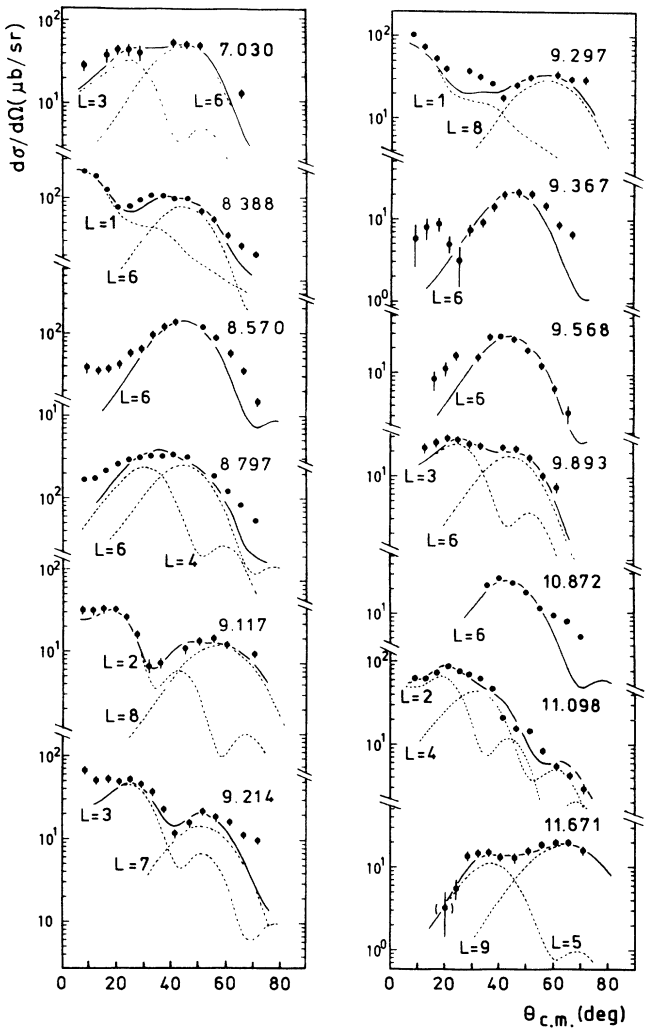

FIG. 8. Experimental angular distributions for $L \geq 6$ states and doublet states. For a doublet state, the DBWA calculations of the assumed components are shown by the dotted lines, while the solid line represents the sum.

confirmed by (p,p'γ) reactions at $E_p=12$ MeV (Ref. 4) and at $E_p=7-9$ MeV (Ref. 5). We also judge these states to be 0^+ by the oscillatory pattern of the angular distributions (see Fig. 2) and by the existence of this level in the (α,α') spectra. It is interesting to note that these states are quite weakly excited in the present experiment in comparison with the results of the experiments at lower incident energies.[4,5] At $E_p=12$ MeV, the cross section of the 4.284 MeV state was about one-tenth that of the first 2^+ state.[4] In the present experiment, however, the ratio is only 1:200. Since the direct excitation process becomes dominant at a higher incident energy, this fact is consistent with the suggested 2p-2h nature of these states.[10,16]

The corresponding 0^+ states have been systematically observed in the nuclei with an $N=28$ neutron closed shell, i.e., ^{52}Cr and ^{54}Fe, by the same (p,p') reaction.[34] As shown in Table III, the trend of lower excitation energies and higher fractions of EWSR is clear as the proton number deviates from the $Z=20$ closed shell. This fact indicates a good shell closure in the ground state of ^{48}Ca.

B. Low-spin unnatural parity states

Several states which were clearly observed in the (p,p') reaction were not identified or scarcely observed (category C in Table I) in the (α,α') spectra. These states are strong candidates for unnatural parity states. One of them is the 1^+ state at 10.2 MeV,[31,35–37] which

TABLE III. Excitation energies and EWSR fractions (S) of the first and the second excited 0^+ states in $N=28$ neutron closed-shell nuclei.

		^{48}Ca	^{52}Cr[a]	^{54}Fe[a]
0_1^+	E_x (MeV)	4.284	2.647	2.561
	S (%)	0.13	0.29	0.55
0_2^+	E_x	5.461	4.738	4.292
	S	0.34	1.20	1.26

[a]Reference 34.

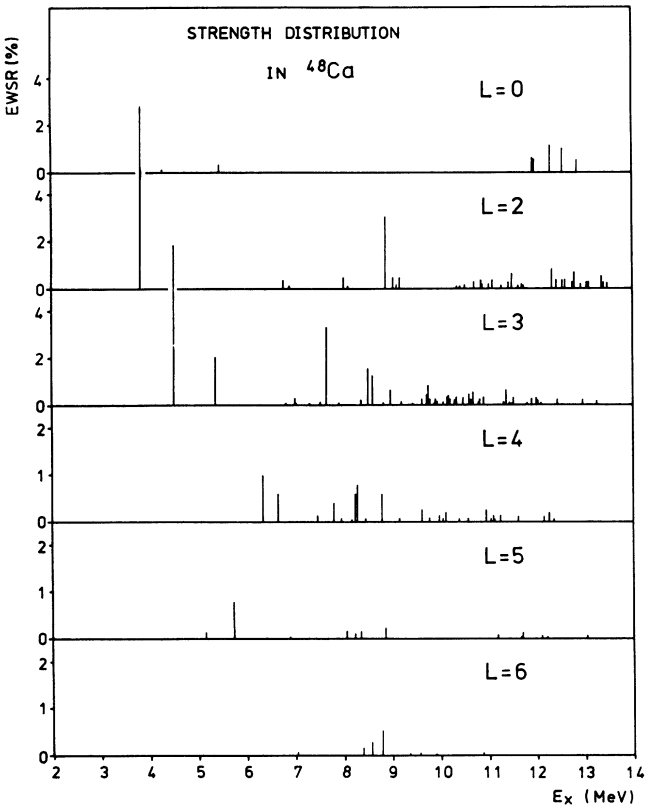

FIG. 9. Distribution of the EWSR percentages found in the ^{48}Ca(p,p') reaction.

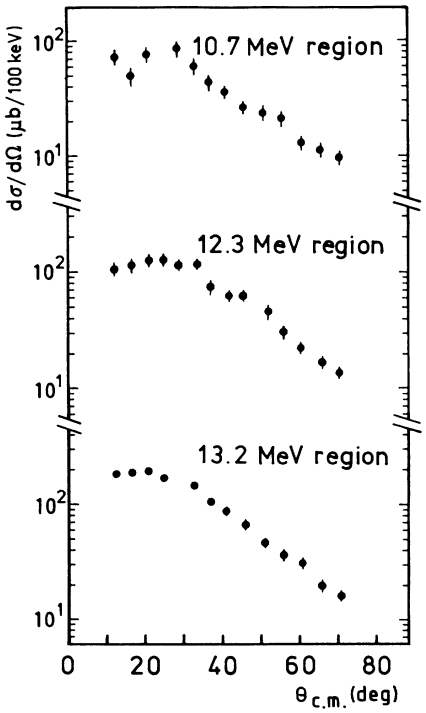

FIG. 10. Angular distribution of the background counts which appear above $E_x = 10$ MeV. The differential cross section per 100 keV is plotted for the three regions indicated above.

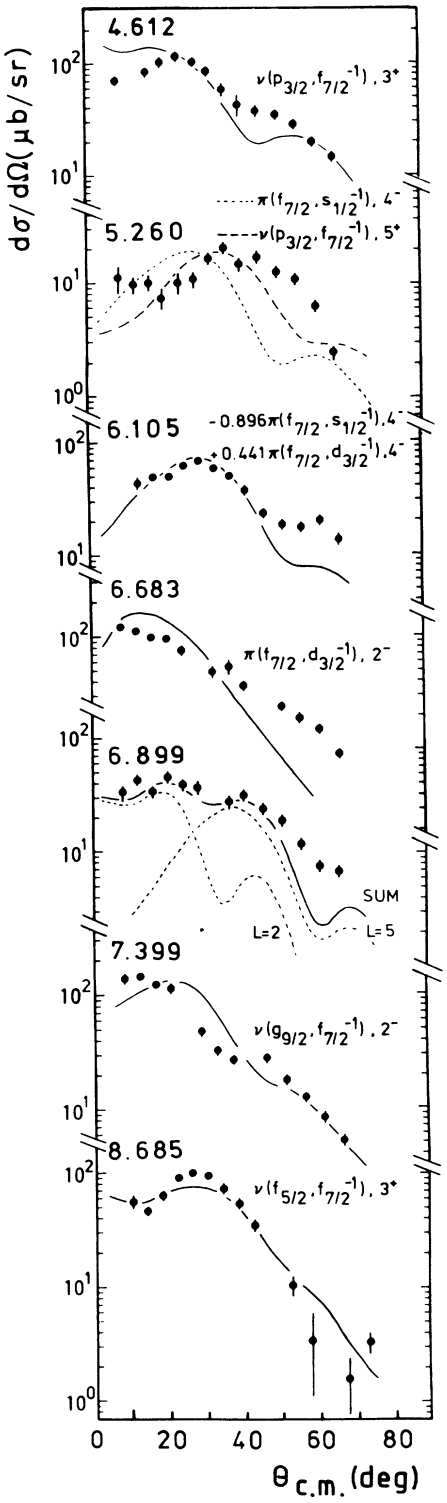

FIG. 11. Angular distributions for the low-lying unnatural parity states. The lines are the results of microscopic DWBA calculations, except for the 6.899 MeV state. For computational details, see text.

TABLE IV. Single p-h configurations in ^{48}Ca, whose single p-h energies are below 11 MeV. The single p-h energies are calculated from the binding energies given in Ref. 14.

Configuration	$E_{s\,\mathrm{ph}}$ (MeV)	Magnetic							Electric						
$\nu(2p_{3/2},f_{7/2}^{-1})$	4.80				3^+		5^+				2^+		4^+		
$\nu(2p_{1/2},f_{7/2}^{-1})$	6.82				3^+								4^+		
$\nu(2p_{3/2},2s_{1/2}^{-1})$	8.49			2^-					1^-						
$\nu(2p_{3/2},d_{3/2}^{-1})$	8.50	0^-		2^-					1^-		3^-				
$\nu(f_{5/2},f_{7/2}^{-1})$	8.76		1^+		3^+		5^+				2^+		4^+		6^+
$\nu(g_{9/2},f_{7/2}^{-1})$	8.82			2^-		4^-		6^-	8^-	1^-		3^-		5^-		7^-
$\nu(2p_{1/2},2s_{1/2}^{-1})$	10.51	0^-								1^-					
$\nu(2p_{1/2},d_{3/2}^{-1})$	10.52			2^-						1^-					
$\pi(f_{7/2},2s_{1/2}^{-1})$	5.64					4^-						3^-			
$\pi(f_{7/2},d_{3/2}^{-1})$	6.01			2^-		4^-						3^-		5^-	
$\pi(f_{7/2},d_{5/2}^{-1})$	9.79			2^-		4^-		6^-		1^-		3^-		5^-	
$\pi(2p_{3/2},2s_{1/2}^{-1})$	10.06			2^-						1^-					
$\pi(2p_{3/2},d_{3/2}^{-1})$	10.43	0^-		2^-						1^-		3^-			

became a standard of 1^+ states around this mass region,[34,38,39] because it is the strongest 1^+ state (for the angular distribution, see Fig. 3). As described in detail in the previous paper,[31] this state observed at $E_x = 10.210$ MeV was clearly identified to be a 1^+ state by a comparison of both (p,p') and (α,α') spectra. The observed strength was one-fourth of the pure $\nu(f_{5/2},f_{7/2}^{-1})_{1^+}$ excitation.

Here we will try to assign the spins and parities of the candidates for unnatural parity states through microscopic DWBA analysis. The DWBA calculation was performed using a computer code DWBA83,[40] where knock-on exchange processes are treated exactly. The optical potential used is the same as given in Table II and the effective-two-body interaction used is the M3Y.[41] Single particle wave functions were calculated in a Woods-Saxon well of radius $R = 1.25A^{1/3}$ fm, diffuseness $a = 0.6$ fm, and a spin-orbit force of 6 MeV. The binding energies of single-particle states were taken from Ref. 14.

Theoretical predictions were also of great help in the identification process. Here we refer to a RPA calculation by Jaffrin and Ripka[14] (JR calculation) for the odd-parity states, and to a shell model calculation by Muto[17] for the even-parity states.

The p-h configurations with single p-h energies below 11 MeV and the expected spin and parity are tabulated in Table IV. The obtained angular distributions of the candidate for unnatural parity states and the fit by DWBA calculation are shown in Fig. 11. The results of the present experiment are compared with those of previous data in Table V.

TABLE V. A comparison of possible low-spin magnetic excitations in ^{48}Ca.

(p,p'γ)[a]		^{48}K β decay[b]		(p,p') $E_p = 25$–40 MeV[c]		(p,p') $E_p = 160$ MeV[d]		(e,e')[e]		Present work	
E_x (MeV)	J^π	E_x	J^π	E_x	L	E_x	L	E_x	J^π	E_x	J^π
4.613	3^+			4.608	(4)	4.613		4.608	3^+	4.612	3^+
5.147	$5^\pm$	5.146	4^-	5.147	5	5.147	4	5.147	5^+	5.147	5^-[f]
		5.252	4^-	5.252				5.252	(4^-)	5.260	(5^+)
				6.104		6.104	4	6.105	4^-	6.105	(4^-)
		6.685	2^-					6.689		6.683	2^-
		6.895	2^-	6.897	5	6.897	$\gtrsim 3$	6.893	(5^+)	6.899	$(2^- + 5^+)$[g]
				7.401	(3)			7.397	(4^-)	7.399	(2^-)
				8.680	(3,4)					8.685	(3^+)

[a]References 6 and 7.
[b]Reference 33.
[c]Reference 1.
[d]Reference 3.
[e]Reference 12.
[f]Observed in the (α,α') spectra.
[g]See text.

1. 4.612 MeV state

This state has been identified to be $J^\pi=3^+$ in the (p,p'γ) experiments.[6,7] Judging by the single p-h energy shown in Table IV, the main configuration of this state is inferred to be $\nu(p_{3/2},f_{7/2}^{-1})$. The calculated angular distribution assuming the pure configuration was best fitted to the obtained distribution with a normalization factor of 0.33. This value is in good agreement with that of an (e,e') experiment,[12] which gives a value of 0.28.

2. 5.260 MeV state

The first maximum in the angular distribution is fitted by an L transfer of about 5. Thus, possible J^π values are 4^-, 5^+, and 6^-. The $J^\pi=4^-$ assignment was suggested by a β-decay experiment from ^{48}K.[33] The result of the (e,e') experiment[12] was consistent with the proposal, but the assignment was not confirmed because of insufficient quality of the data. The JR calculation predicts a $J^\pi=4^-$ state mainly of $\pi(f_{7/2},s_{1/2}^{-1})$ configuration at $E_x=5.5$ MeV, while a shell model calculation by Muto predicts a $\nu(p_{3/2},f_{7/2}^{-1})$, $J^\pi=5^+$ state at $E_x=5.8$ MeV.

A microscopic DWBA calculation has been performed assuming the above two configurations. As shown in Fig. 11, the angular distribution is not fitted by the $\pi(f_{7/2},s_{1/2}^{-1})$, $J^\pi=4^-$ calculation, but is rather well fitted by the 5^+ calculation assuming $\nu(p_{3/2},f_{7/2}^{-1})$. Here we tentatively propose $J^\pi=5^+$ for this state. However, the normalization factor of 0.05 required to fit the data is much smaller than the value of 0.33 for the 4.612 MeV, 3^+ state of the same configuration.

3. 6.105 MeV state

This level shows an angular distribution similar to that of 6.345 MeV, 4^+ state, although the second maximum is rather large. In the (p,p') reaction the observed strength was about one-ninth that of the 6.345 MeV, 4^+ state. On the other hand, in the (α,α') spectra this state was hard to distinguish. The (e,e') reaction[12] suggests that the J^π of this state is 4^-. Our result is in accordance with their suggestion.

The excitation energy indicates that the dominant configurations of the state are $\pi(f_{7/2},s_{1/2}^{-1})$ and $\pi(f_{7/2},d_{3/2}^{-1})$, which have very close p-h energies to each other (see Table IV). The JR calculation predicts two 4^- states at $E_x=5.5$ and 5.8 MeV, and it also predicts that the former state should be excited rather strongly by the (p,p') reaction. By assuming a configuration of the former state, namely

$$|4^-\rangle=-0.896\pi(f_{7/2},s_{1/2}^{-1})_{4^-}+0.441\pi(f_{7/2},d_{3/2}^{-1})_{4^-}\ , \tag{6}$$

a DWBA calculation was performed and the result is shown in Fig. 11. The normalization factor of 0.8 was needed to fit the data.

4. 6.683 MeV state

This state is suggested to be a 2^- state in the β-decay experiment.[33] The 6.683 MeV state forms a triplet with the 6.612 and 6.648 MeV states (see Fig. 1). Thus, attention was paid to the analysis of the spectra. The obtained angular distribution of the 6.683 MeV state decreases smoothly and is quite similar to that of a 2^- state at 6.75 MeV in ^{40}Ca.[25] The JR calculation predicts the first 2^- state at $E_x=6.3$ MeV, which has almost a pure $\pi(f_{7/2},d_{3/2}^{-1})$ configuration. The result of microscopic DWBA calculation is fitted to the data with the normalization factor of 0.06.

5. 6.899 MeV state

The β-decay experiment[33] suggests a $J^\pi=2^-$ level at $E_x=6.895$ MeV, while the (e,e') experiment[12] favors a 5^+ state at 6.893 MeV. In the (α,α') spectra it was difficult to recognize this state partly because this state was excited very weakly and partly because a contaminant peak overlapped in the spectrum of $\theta_{\rm lab}=13°$. The proton angular distribution obtained for the state shows two local maxima, which are tentatively fitted by the $L=2$ and 5, respectively in the collective-model DWBA analysis. Taking the usual similarity of the peak positions between 2^+ and 2^- states, and also the 5^- and 5^+ states into consideration, our data seem to be consistent with the assumption that this state is the mixture of a 2^- and a 5^+ state.

6. 7.399 MeV state

This state was suggested to be a 4^- state in the (e,e') experiment.[12] In our experiment the angular distribution decreases like the 6.683 MeV, 2^- state, as shown in Fig. 11. Thus we tentatively give a 2^- assignment. Table IV suggests that several configurations can make 2^- states at around $E_x=6$–9 MeV. The JR calculation predicts the second 2^- state with the main configuration of $\nu(g_{9/2},f_{7/2}^{-1})$ at $E_x=8.4$ MeV. The experimental angular distribution is fitted well by a calculation assuming the above configuration, where a normalization factor of 0.06 was necessary to fit the data.

An additional 2^- state is suggested at 10.000 MeV in an (e,e') experiment.[42] We could not, however, observe a corresponding state.

7. 8.685 MeV state

This state is a newly discovered candidate for an unnatural parity state. Judging from the shape of the angular distribution, and also from the excitation energy, it is inferred that this state is a 3^+ state which is expected at 8.85 MeV and has a main configuration of $\nu(f_{5/2},f_{7/2}^{-1})$.[17] As shown in Fig. 11, a fairly good fit to the data is obtained by assuming $J^\pi=3^+$ and a pure $\nu(f_{5/2},f_{7/2}^{-1})$ configuration where a normalization factor of 0.24 is used. It should be noted that this factor is in good accordance with that for the 10.2 MeV, 1^+ state (0.25) having the same main configuration of $\nu(f_{5/2},f_{7/2}^{-1})$.[31]

C. Strength distribution

Strength distributions show directly concentrations of various multipolarities. Thus, they are important in the analysis of various properties of a collective motion, especially of a giant resonance. In the distribution shown in Fig. 9, suspected unnatural parity states are excluded. Consequently, the distributions are expected to correspond to those of isoscalar natural parity states. Of course, there still remains ambiguities of the spin-parity assignment for some of the weakly excited states and also for the states with $E_x > 12$ MeV, because we could not clearly assign them in the (α,α') spectra. It often happens that the feature of a strength distribution is clearly seen by plotting the strength in the form of a cumulative sum, and this is shown in Fig. 12.

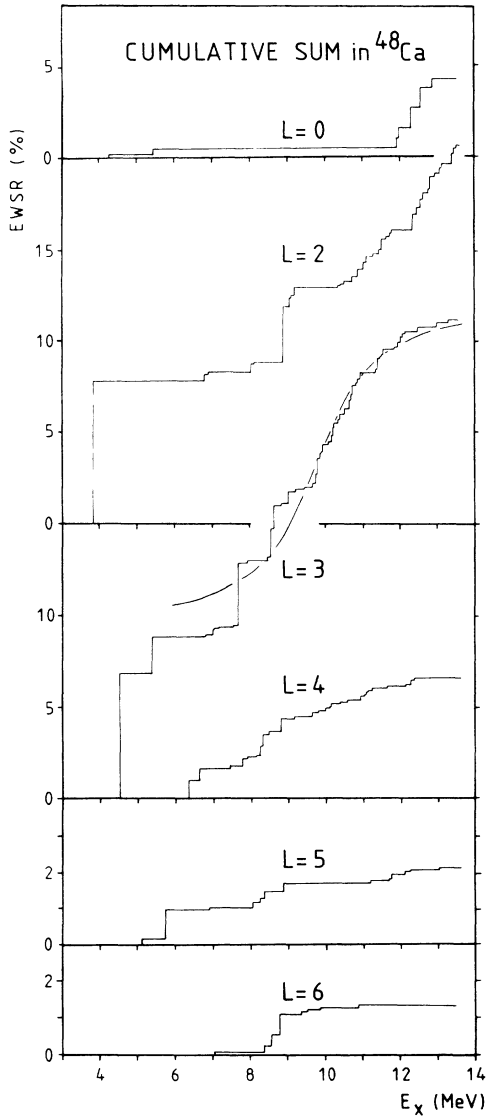

FIG. 12. Cumulative sum of EWSR fraction for $L=0$, 2, 3, 4, 5, and 6 strengths.

1. $L=0$ strength

In addition to the low-lying 0^+ states, which were described earlier, five states above $E_x=11.9$ MeV showed oscillatory angular distributions, and they were also well fitted by the DWBA 0^+ calculation (see Fig. 2). As shown in Fig. 9, these five states cluster together and the sum of the EWSR fractions is about 4%. The cumulative sum shown in Fig. 12 increases rapidly above $E_x=11.9$ MeV. If this feature is compared with that of the $L=2$ giant quadrupole resonance (GQR) described later, it is suggested that these states are the lower tail of the giant monopole resonance (GMR).[43,44] It may seem that excitation energies of these states, even if they are the tail part of the GMR, are very low, because for an $A=48$ nucleus the centroid energy of the GMR is predicted to be at $E_x=22$ MeV by a simple relation $E_x=80A^{-1/3}$ MeV, which is derived phenomenologically for well established GMR's in medium and heavy nuclei.[43,44] Recently, (α,α') experiments including a measurement at 0° identified the GMR's in very light nuclei, ^{24}Mg and ^{28}Si.[45,46] The centroids were both at about $E_x=17.5$ MeV, and the strengths were quite fragmented. These energies are much lower than the values predicted by the relation $E_x=80A^{-1/3}$ MeV ($E_x=28$ and 26 MeV for ^{24}Mg and ^{28}Si, respectively). By interpolation between the centroid energies for these light nuclei and the well-known values for medium and heavy nuclei, the centroid of the GMR is expected at about $E_x=17$ MeV in ^{48}Ca. Then, it is reasonable to observe the tail part of the GMR at an excitation energy above $E_x=12$ MeV and to find 4% of the EWSR between this energy and 13.6 MeV. Among the calcium isotopes, 30% of the EWSR has been reported in ^{40}Ca at around $E_x=14.4$ MeV.[47]

The isoscalar GMR has been usually identified using an (α,α') experiment in order to distinguish it from the isovector giant dipole resonance (GDR) which exists in nearly the same energy region.[18,43] Quite recently, however, the identification of the GMR by an (α,α') reaction has been questioned. Peterson suggested theoretically that the GDR can show a similar angular distribution to the GMR in an (α,α') experiment, if the effect of Coulomb excitation is taken into account properly.[48] In the present experiment, however, $L=0$ states forming the GMR could be distinguished from $L=1$ states by the (p,p') reaction, in which the angular distributions were out of phase with each other. Thus, we can be quite certain that the GMR really exists.

From our direct observation of discrete 0^+ states in the GMR, it is clear that the strength of the GMR is fragmented into many levels, at least in the tail part. As seen in Fig. 9, it is also clear that GMR strengths are intermingled with GQR strengths and the trend that the excitation energy of the GMR is lower in the medium light nuclei than the systematics ($E_x=80A^{-1/3}$ MeV) would suggest is supported by our experiment.

The states at $E_x=11.013$ and 11.550 MeV showed oscillatory angular distributions (see Fig. 2). The angular distributions, however, were out of phase with that of a $J^\pi=0^+$ calculation, which is shown by a dotted line.

Although we cannot discuss the nature of these states in detail, these states can be the 0^- states of a $\pi(2p_{1/2},2s_{1/2}^{-1})$ configuration which is predicted at $E_x=12$ MeV by a RPA calculation.[49]

2. $L=1$ strength

Various 1p-1h configurations can make $J^\pi=1^-$ states at $E_x=8.5$–10.5 MeV (see Table IV). Up to now, however, only one 1^- state has been established at $E_x=6.614$ MeV.[13,33] In the present experiment about 20 levels were empirically assigned to have $L=1$ transitions, and some of them were identified to be $J^\pi=1^-$ by a clear observation in (α,α') spectra. Unfortunately, the result of $L=1$ collective model DWBA calculations could not fit the data well. Therefore deformation parameters were not obtained. The differential cross sections at $\theta_{\text{c.m.}}=15°$ are shown in Fig. 13. As seen in the figure, strengths fairly concentrate at around $E_x=9.5$ MeV. Among them, the 9.461 and 9.537 MeV states were clearly observed in both the (p,p') and the (α,α') reactions. In the (p,p') spectra the 9.537 MeV state was about 2 times more strongly excited than the 9.461 MeV state, while the strength was reversed in the (α,α') spectra. This fact suggests that the p-h configurations of these states are different. Presumably the main p-h configuration(s) of the 9.537 MeV state is (are) accompanied by a spin flip process and Table IV indicates that two configurations $\nu(p_{3/2},d_{3/2}^{-1})$ and $\pi(p_{3/2},d_{3/2}^{-1})$ can be the candidates. According to the JR calculation, a $J^\pi=1^-$ state mainly of the above p-h configurations is predicted at $E_x=8.5$ MeV.

3. $L=2$ strength

As seen from Fig. 9, the 2^+ strength is categorized into three groups, i.e., the low-lying state at $E_x=3.8$ MeV, several states at around $E_x=9$ MeV, and many clustering states at above $E_x=10.5$ MeV.

The 3.8 MeV state exhausts 7.8% of the EWSR and the states around $E_x=9$ MeV exhaust 5.1% in total. According to Table IV, two configurations $\nu(p_{3/2},f_{7/2}^{-1})$ and $\nu(f_{5/2},f_{7/2}^{-1})$ with p-h energies of 2.1 and 8.2 MeV, respectively, can form 2^+ states below $E_x=10$ MeV. These p-h energies suggest that the first 2^+ state at $E_x=3.832$ MeV is attributed mainly to the former configuration, while the states at around 9 MeV are attributed mainly to the latter. The speculation should be confirmed by comparing the excitation strengths in the (p,p') and (α,α') reactions, because the $f_{7/2}\rightarrow f_{5/2}$ transition is accompanied by a spin flip process, while the $f_{7/2}\rightarrow p_{3/2}$ transition is not. In the (p,p') reaction the strength of the 8.883 MeV state, the main 2^+ state around $E_x=9$ MeV, is one-sixth that of the 3.832 MeV state. On the other hand, in the (α,α') reaction the ratio is one-sixteenth. The 8.883 MeV state is largely hindered in the (α,α') reaction.

The 2^+ strength above $E_x=10.5$ MeV is fragmented into many states; each state exhausts at most 1% of the EWSR. Similar clustering of $L=2$ states is observed in ^{208}Pb above $E_x=7$ MeV.[19] These states are thought to be the lower tail of the GQR observed systematically by (p,p') and (α,α') experiments,[43] because the centroid of the GQR in ^{48}Ca is expected at $E_x=17.3$ MeV according to the empirical systematics $E_x=63A^{-1/3}$ MeV. The sum total of the strength is 7.8% of the EWSR. This value should be considered to be the lower limit, because some of the weak levels with less than 0.1% of the EWSR could not be analyzed due to the high level density above 10 MeV. As shown in Fig. 12, the cumulative sum increases continuously in the region between $E_x=10.5$ and 13.6 MeV. It seems that the sum is still increasing at the higher excitation energy.

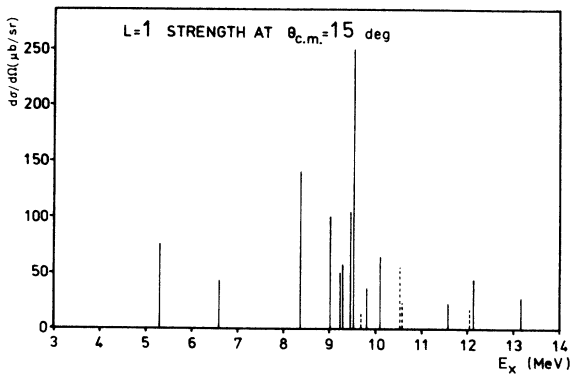

FIG. 13. Differential cross sections of $L=1$, probably of $J^\pi=1^-$ states at $\theta_{\text{c.m.}}=15°$. The states for which the identification is less certain are indicated by the dotted lines.

4. $L=3$ strength

According to a simple harmonic-oscillator shell model, $L=3$ strengths are predicted at excitations of $1\hbar\omega$ and $3\hbar\omega$. From the location of the observed strength, all $L=3$ levels observed in the present experiment are those of $1\hbar\omega$ excitations. As seen from Fig. 9, the strength is roughly divided into two groups; they are two low-lying collective states and the LEOR above $E_x=7$ MeV. The LEOR is observed in many nuclei with $A=27$,[50] $50\leq A\leq 54$,[34] $66\leq A\leq 197$,[51] and recently in ^{208}Pb.[19]

The existence of two low-lying 3^- states at $E_x=4.507$ and 5.370 MeV is attributed to the existence of two configurations, $\pi(f_{7/2},d_{3/2}^{-1})$ and $\pi(f_{7/2},s_{1/2}^{-1})$, which are very close in their single p-h energies (see Table IV). In the (p,p') reaction the cross section of the 5.370 MeV state was about one-fourth that of the 4.507 MeV state (see Table I), while in the (α,α') reaction the ratio was one-sixth. Then it is inferred that the $\pi(f_{7/2},s_{1/2}^{-1})$ configuration is rather dominant in the first 3^- state, $\pi(f_{7/2},d_{3/2}^{-1})$ in the second 3^- state, because the $d_{3/2}\rightarrow f_{7/2}$ transition is accompanied by a spin flip process. The result is consistent with the JR calculation,[14] and with the result of an (e,e') experiment.[12] The ratio of excitation strengths between the 4.507 MeV state and a prominent state at 7.661 MeV was nearly the same in both (p,p') and (α,α') experiments.

The LEOR region ranges from $E_x=7$ to 13 MeV, where 17% of the EWSR strength is fragmented into more than 40 levels. The envelope of the LEOR exhibits

a resonancelike shape (see Fig. 9). The feature is more clear in the cumulative sum shown in Fig. 12. The sum starts to increase from $E_x=7$ MeV and increases considerably between $E_x=9$ and 11 MeV. The increase, however, is small above $E_x=12$ MeV. In order to know the width Γ and the central value of the excitation energy E_0, the cumulative sum was fitted to the integrated Breit-Wigner function

$$Y(E)=Y_0[(1/\pi)\tan^{-1}(E-E_0)/(\Gamma/2)+\tfrac{1}{2}]\ , \qquad (7)$$

where Y_0 is the integrated strength. The result of the fit is shown in Fig. 12 by the solid line and obtained values for E_0 and Γ are compared in Table VI with those of other closed-shell nuclei, ^{90}Zr and ^{208}Pb.[19] The values for ^{48}Ca given in the previous paper[19] are slightly corrected, because the analysis is extended to a higher excitation energy and probable unnatural parity states are excluded. The E_0 value for ^{48}Ca is 9.7 MeV, while it decreases for larger mass nuclei. The excitation energy of a GR is usually assumed to be proportional to $A^{-1/3}$,[52] Then the quantity $E_0A^{1/3}$ gives a measure of whether the E_0 value for a nucleus is large or not, independent of the mass number. Column 3 of Table VI shows these values. All of these three nuclei have $E_0A^{1/3}$ values larger than the empirically accepted value of 30,[18] and among them, ^{48}Ca has the largest value of 35. According to the high resolution (p,p') reaction on nearby nuclei, ^{50}Ti, ^{52}Cr, and ^{54}Fe,[34] those values are 28, 27, and 29, respectively. Thus it is concluded that the value of ^{48}Ca is extremely large.

Theoretically it is expected that the width Γ of a GR is proportional to E_0^2.[53] Thus the quantity Γ/E_0^2 gives a good measure of the "intrinsic width" of a GR in a nucleus. From the above values of Γ and E_0, we obtain $\Gamma/E_0^2=2.4\times10^{-2}$ for the LEOR in ^{48}Ca. Among the three nuclei shown in Table VI, the value of the "intrinsic width" is largest in ^{90}Zr and smallest in ^{208}Pb.

5. $L=4$ strength

In ^{90}Zr a number of $J^\pi=4^+$ states were observed in the same excitation region as the LEOR.[54] The same is true in ^{48}Ca, where 27 levels show the angular distribution of $L=4$, and the EWSR percentage amounts to 6.5% of the isoscalar hexadecapole mode. As seen from the strength distribution (Fig. 9) and the cumulative sum (Fig. 12), the strengths are found in the region between $E_x=6$ and 12 MeV. In the harmonic-oscillator shell-model picture, excitations of $0\hbar\omega$, $2\hbar\omega$, and $4\hbar\omega$ are expected for $L=4$ strength. From the location of strengths, the observed 4^+ states are mainly of $0\hbar\omega$. In the $0\hbar\omega$ excitation, only three 1p-1h transitions of $\nu(p_{3/2},f_{7/2}^{-1})$, $\nu(p_{1/2},f_{7/2}^{-1})$, and $\nu(f_{5/2},f_{7/2}^{-1})$ are expected to form 4^+ states in ^{48}Ca; however, 27 4^+ states were observed experimentally. It is clear that we cannot account for the number without considering the coupling of the 4^+ states with 2p-2h states, as was suggested for the fragmentation of the LEOR.[19]

TABLE VI. Properties of low-energy octupole resonance in ^{48}Ca, ^{90}Zr, and ^{208}Pb.

	E_0 (MeV)	$E_0A^{1/3}$	Γ (MeV)	Γ/E_0^2
^{48}Ca	9.7	35.4	2.3	2.4×10^{-2}
^{90}Zr[a]	7.2	32.4	1.7	3.3×10^{-2}
^{208}Pb[a]	5.4	31.9	0.5	1.6×10^{-2}

[a]Reference 19.

6. $L=5$ strength

As seen from Figs. 9 and 12, $L=5$ strengths of 1.0%, 0.7%, and 0.4% of the EWSR are found at around $E_x=5.5$, 8.5, and 11.5 MeV, respectively. According to the JR calculation, a 5^- state with the main configuration of $\pi(f_{7/2},d_{3/2}^{-1})$ is expected at $E_x=5.5$ MeV, while states with main configurations of $\nu(g_{9/2},f_{7/2}^{-1})$ and $\pi(f_{7/2},d_{5/2}^{-1})$ are predicted at 8.5 and 9.5 MeV, respectively. These states roughly correspond to the first and second groups of states observed at around $E_x=5.5$ and 8.5 MeV, respectively. The JR calculation predicts transition strengths of 3% and 1.5% of the EWSR for the first and second groups, respectively. These values, however, are roughly twice as large as the observed ones.

7. $L=6$ and higher L strengths

It is strange that no $L=6$ strength has so far been reported in ^{48}Ca. In the present analysis eight states were identified to have an L value of 6 (see Fig. 8). The strength distributions are shown in Fig. 9 and Fig. 12. These states are dominant at backward angles, and some of them are not well resolved at forward angles. As is clear from Table IV, the $\nu(f_{5/2},f_{7/2}^{-1})$ is the only configuration which couples to $J^\pi=6^+$ and it has a 1p-1h energy of about 8.5 MeV. The identification of eight 6^+ states suggests the admixture of other configurations in the states observed. However, it should be noted that three of the strongest ones, i.e., 8.388, 8.570, and 8.797 MeV states, are all concentrated at around $E_x=8.5$ MeV, the value of which is the same as the p-h energy of the $\nu(f_{5/2},f_{7/2}^{-1})$ configuration. The (p,p') experiment at $E_p=25$–40 MeV (Ref. 1) assigned $L=5$ transitions to these levels (see Table I), but the angular distributions for these levels have their first maxima characteristic of $L=6$ transitions in our experiment (see Fig. 8).

Among the three states mentioned above, the 8.570 MeV state was suggested to be a 6^- state with the configuration of $\pi(f_{7/2},d_{5/2}^{-1})$ in the (e,e') experiment.[12] Unfortunately, no decisive comment can be made on this issue, because we could not judge the existence or the nonexistence of $L=6$ states in our forward angle (α,α') spectra. As seen from Table IV, two configurations of $\nu(g_{9/2},f_{7/2}^{-1})$ and $\pi(f_{7/2},d_{5/2}^{-1})$ can make 6^- states at around $E_x=9$ MeV. In the top part of Fig. 14, the results of DWBA calculations assuming these configurations are fitted to the data. The calculation assuming the latter configuration fits the data slightly better than the former. A normalization factor of 0.36 was used for the former, while one of 0.23 was used for

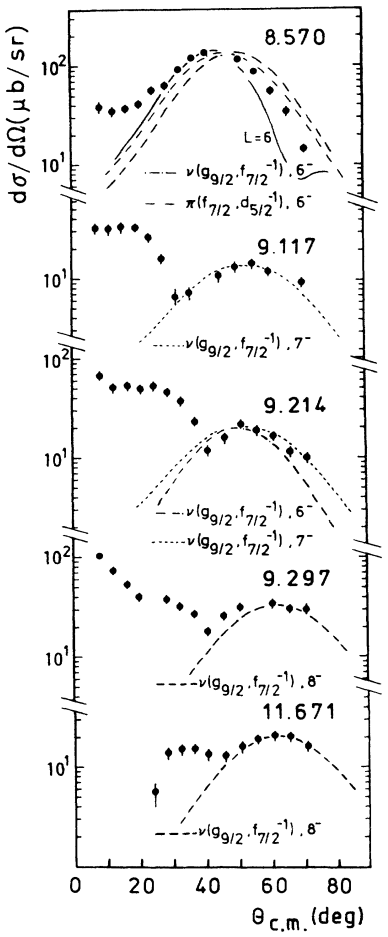

FIG. 14. Fit of DWBA calculations to the observed angular distributions of high-spin states. The solid line for the 8.570 MeV state is a result of collective-model DWBA calculations. Other lines represent the results of microscopic DWBA calculations assuming the indicated configurations.

the latter. The (e,e') experiment tentatively suggested an another 6^- state with the configuration of $\nu(g_{9/2},f_{7/2}^{-1})$ at $E_x=7.95$ MeV. We could, however, observe no large L state around this excitation energy.

Possible high-spin states were found at 9.117, 9.214, 9.297, and 11.671 MeV. Each of these states overlaps with a state having a smaller L transfer, and the reliable data on the angular distribution could be obtained only at backward angles. The peak positions were fitted by a collective-model DWBA calculation in order to obtain some idea about the spin values for the states. The L transfers of 8, 7, 8, and 9, respectively, were obtained for these states (see Fig. 8). The neutron $(g_{9/2},f_{7/2}^{-1})$ multiplet states are expected at around $E_x=9$ MeV in ^{48}Ca. Among the multiplet are the high-spin "stretched" or "nearly stretched" states of 8^-, 7^-, and 6^- (see Table IV). Microscopic DWBA calculations have been performed for these states and are compared with the data as shown in Fig. 14. The 9.297 MeV state is well fitted by the 8^- calculation, the 9.117 MeV state by the 7^- calculation, and the 9.214 MeV state either by 6^- or 7^- calculations. The 11.671 MeV state is also well fitted by the 8^- calculation. Some of these states have been observed in the (p,p') experiment at $E_p=160$ MeV,[3] and also in the (e,e') experiment.[12] Possible correspondence among the data is shown in Table VII. It is strange that a $J^\pi=8^-$ state which is claimed to exist at 9.95 MeV in the (e,e') experiment is not observed in both the present and the $E_p=160$ MeV (p,p') experiments. The 11.671 MeV state is a newly discovered high spin state. A peak corresponding to this state is seen in the spectra of the (p,p') experiment at $E_p=160$ MeV,[3] although the authors mentioned nothing of the state.

D. Comparison of the level structure between theory and experiment

In Fig. 15 the level structure obtained in the present experiment is compared with the results of shell model calculations for the natural parity states. The level structure of the negative parity states is taken from the JR calculation[14] and the positive parity states from the calculation of Muto.[17] As described before, the main configurations of several prominent low-lying states were identified by consulting the results of the (α,α') reaction. Probable correspondences of the levels are indicated in the figure by the dotted lines. In the high excitation region, however, the experimental results are not accounted for by the calculations. The experimental strengths are more fragmented than the results of the calculations.

It is emphasized that the fragmentation of a state is caused by the mixing with states having a 2p-2h na-

TABLE VII. Comparison of excitation energy and assignment for the high-spin states.

Present work		(p,p') $E_p=160$ MeV[a]		(e,e')[b]	
E_x	J^π	E_x	J^π	E_x	J^π
9.117	(7^-)			9.138	8^-
9.214	$(6^-,7^-)$	9.229	$8^\pm$		
				9.276	8^-
9.297	(8^-)	9.307	$8^\pm$		
				9.953	8^-
11.671	(8^-)				

[a]Reference 3.
[b]Reference 12.

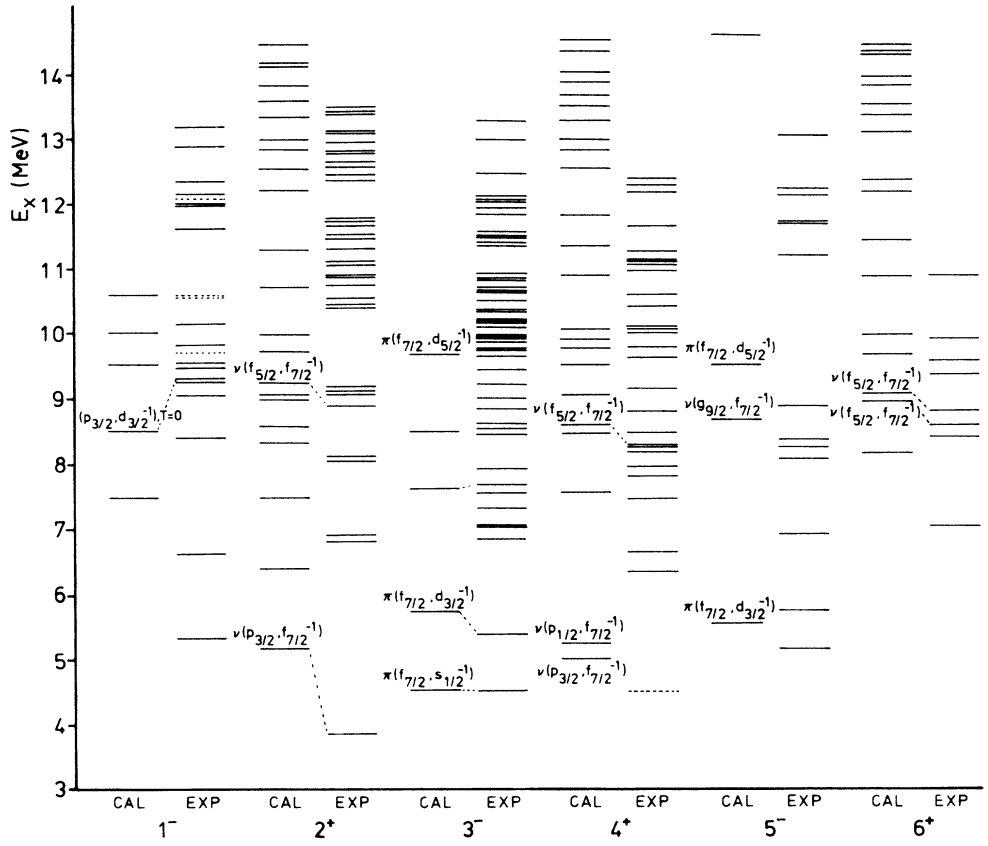

FIG. 15. Comparison between the results of shell model calculations and the results of the present experiment for the natural parity states. The calculated odd-parity and even-parity states are taken from Refs. 14 and 17, respectively. The dominant configuration of a state suggested by the calculation is shown and the probable correspondence with the observed state is indicated.

ture,[53] and our data on the fragmentation of the LEOR support the explanation.[19] Recently, a shell model calculation which includes 2p-2h configurations and treats the symmetry of isospin properly has been performed for the negative parity states.[55] In Fig. 16 the calculated result is compared with the experiment for the isoscalar octupole strength. The fragmentation of the LEOR is described well and the overall correspondence is very good, except for the strong state at $E_x = 10.5$ MeV. The close agreement suggests that the calculation including 2p-2h configurations is essential in understanding the fine structure of the high excitation region of a nucleus.

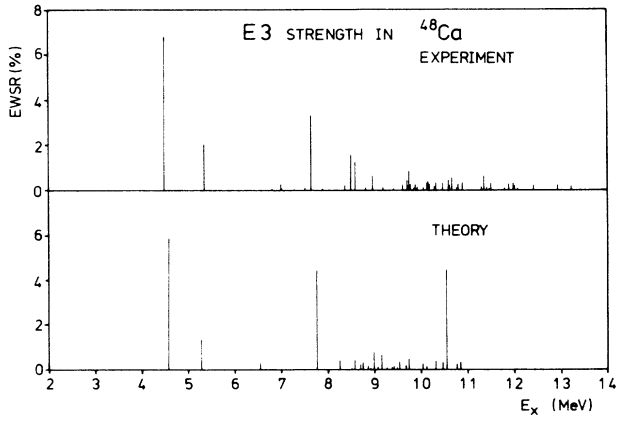

FIG. 16. Comparison of the distribution of $J^\pi = 3^-$ states between the result of a shell model calculation (Ref. 55) and the result of the present experiment.

V. SUMMARY AND CONCLUSION

The nuclear structure of ^{48}Ca was studied up to $E_x = 13.6$ MeV through a proton inelastic scattering experiment at $E_p = 65$ MeV with a resolution of around 15 keV. The high resolution experiment performed at relatively high proton energy and for a wide range of angles enabled us to determine L values of states with less uncertainty. The angular distributions of some of the levels which are claimed to have small L values in the 25–40 MeV (p,p′) reaction[1] and to have large L values at $E_p = 160$ MeV were well fitted by the sum of small and large L values. Many states were identified to be natural parity states by the comparison of the (p,p′) spectra with the (α,α') spectra. The collective-model DWBA analysis has been carried out, and the deformation lengths, βR's, were extracted. Several states were identified to be candidates for unnatural parity states by their lack of observation in the (α,α') spectra. The

values of spin and parity were deduced for each of these states by comparing the angular distributions obtained in the experiment with the results of a microscopic DWBA calculation.

Because of the high resolution of this experiment, the LEOR, the tail part of the GQR, and the GMR were observed as clusters of discrete levels with $L=3$, 2, and 0, respectively. The width of each level was not wider than the experimental energy resolution, although these levels were situated in the excitation region above the neutron separation energy ($S_n=9.94$ MeV for ^{48}Ca). This fact suggests that the natural decay width is much smaller than 15 keV. The levels forming giant resonances, i.e., LEOR, GQR, and GMR, were found to mingle with each other in a wide region of excitation energy in ^{48}Ca. Then it seems that the usual technique of observing the whole resonance as a bump is not appropriate to locate each of these resonances separately. It is suggested that the tail part of the GMR coincides in its excitation energy with that of a strongly excited GQR whose center is expected at around $E_x=65A^{-1/3}$ MeV. This fact strongly supports the recent results that for light nuclei the excitation energy of the GMR is much lower than the value predicted by the simple relation $E_x=80A^{-1/3}$ MeV, which is derived phenomenologically for medium and heavy nuclei. Furthermore, we believe that the usual lack of GMR strength observed in light nuclei is due to the problems involved in unfolding the GMR, GQR, continuum, and other multipole strengths. Since the $L=3$ strengths have been extracted quite cleanly, the width Γ, as well as the excitation energy E_0 of the LEOR, could be obtained with less uncertainty compared with previous works. It was found that the excitation energy of the LEOR is rather high in ^{48}Ca.

In conclusion, the (p,p′) experiment performed at $E_p=65$ MeV with a good-resolution detection system made it possible to extract the properties of about 200 states in ^{48}Ca.

ACKNOWLEDGMENTS

We would like to express our gratitude to all the staff at RCNP, Osaka University, for making this work possible. They are grateful to Dr. K. Muto (Tokyo Institute of Technology) and Dr. K. Arita (Aoyama Gakuin University) for their valuable discussions and shell-model calculations. Thanks are also due to Dr. T. Yamagata (Konan University), and Dr. P. F. Bortignon (Legnaro, Padova) for their discussions on giant resonances. They are grateful to Mr. I. Sugai of INS, the University of Tokyo, for preparing the target foil. One of the authors (Y.F.) expresses his gratitude to Prof. H. Matsuda and Prof. T. Matsuo (Osaka University) for their encouragement. The experiment was performed at RCNP under Grant No. 11A09.

[1]C. R. Gruhn, T. Y. T. Kuo, C. J. Maggiore, and B. M. Preedom, Phys. Rev. C **6**, 944 (1972).
[2]G. S. Adams, Th. S. Bauer, G. Igo, G. Pauletta, C. A. Whitten, Jr., A. Wriekat, G. W. Hoffmann, G. R. Smith, and M. Gazzaly, Phys. Rev. C **21**, 2485 (1980).
[3]R. E. Segel, K. E. Rehm, P. Kienle, J. R. Comfort, and D. W. Miller, Phys. Rev. C **29**, 1703 (1984).
[4]A. Tellez, R. Ballini, J. Delaunay, and J. P. Fouan, Nucl. Phys. **A127**, 438 (1969).
[5]N. Benczer-Koller, G. G. Seaman, M. C. Bertin, J. W. Tape, and Jack R. MacDonald, Phys. Rev. C **2**, 1037 (1970).
[6]J. W. Tape, M. Ulrickson, N. Benczer-Koller, and Jack R. MacDonald, Phys. Rev. C **12**, 2125 (1975).
[7]J. W. Tape, R. Hensler, N. Benczer-Koller, and Jack R. MacDonald, Nucl. Phys. **A195**, 57 (1972).
[8]R. J. Peterson, Phys. Rev. **140**, B1479 (1965).
[9]E. P. Lippincott and A. M. Bernstein, Phys. Rev. **163**, 1170 (1967).
[10]J. H. Bjerregaard, Ole Hansen, O. Nathan, R. Chapman, S. Hinds, and R. Middleton, Nucl. Phys. **A103**, 33 (1967).
[11]R. A. Eisenstein, D. W. Madsen, H. Theissen, L. S. Cardman, and C. K. Bockelman, Phys. Rev. **188**, 1815 (1969).
[12]J. E. Wise, J. S. McCarthy, R. Altemus, B. E. Norum, R. R. Whitney, J. Heisenberg, J. Dawson, and O. Schwentker, Phys. Rev. C **31**, 1699 (1985).
[13]D. E. Alburger, At. Nucl. Data Sheets **45**, 557 (1985).
[14]A. Jaffrin and G. Ripka, Nucl. Phys. **A119**, 529 (1968).
[15]J. B. McGrory, B. H. Wildenthal, and E. C. Halbert, Phys. Rev. C **2**, 186 (1970).
[16]P. Federman and S. Pittel, Nucl. Phys. **A155**, 161 (1970).
[17]K. Muto and H. Horie, Phys. Lett. **138B**, 9 (1984), and private communication.
[18]A. van der Woude, Kernfysisch Versneller Instituut Report KVI-583, 1986; Prog. Part. Nucl. Phys. **18**, 217 (1987).
[19]Y. Fujita, M. Fujiwara, S. Morinobu, I. Katayama, T. Yamazaki, T. Itahashi, H. Ikegami, and S. I. Hayakawa, Phys. Rev. C **32**, 425 (1985).
[20]H. Ikegami, S. Morinobu, I. Katayama, M. Fujiwara, and S. Yamabe, Nucl. Instrum. Methods **175**, 335 (1981).
[21]Y. Fujita, K. Nagayama, S. Morinobu, M. Fujiwara, I. Katayama, T. Yamazaki, and H. Ikegami, Nucl. Instrum. Methods **173**, 265 (1980); Y. Fujita, K. Nagayama, M. Fujiwara, S. Morinobu, T. Yamazaki, and H. Ikegami, *ibid.* **217**, 441 (1983).
[22]H. Ikegami, in Proceedings of the International Conference on Magnet Technology, Bratislava, 1977, p. 904; H. Ikegami, T. Takayama, M. Fujiwara, I. Katayama, and S. Morinobu, *ibid.*, p. 908.
[23]Y. Fujita, S. Morinobu, M. Fujiwara, I. Katayama, T. Yamazaki, and H. Ikegami, Nucl. Instrum. Methods **225**, 298 (1984), and references therein.
[24]I. Katayama, S. Morinobu, Y. Fujita, M. Fujiwara, T. Yamazaki, and H. Ikegami, Nucl. Instrum. Methods **171**, 195 (1980).
[25]H. Ejiri, M. Sasao, T. Shibata, H. Ohsumi, Y. Fujita, M. Fujiwara, T. Yamazaki, I. Katayama, S. Morinobu, and H. Ikegami, Phys. Rev. C **24**, 2001 (1981).
[26]S. Morinobu, private communication.
[27]P. D. Kunz, DWUCK, a DWBA computer program, University of Colorado (unpublished).
[28]T. Yamagata, private communication.
[29]G. R. Satchler, Part. Nucl. **5**, 105 (1973).

[30]H. Sakaguchi, M. Nakamura, K. Hatanaka, A. Goto, T. Noro, F. Ohtani, H. Sakamoto, H. Ogawa, and S. Kobayashi, Phys. Rev. C **26**, 944 (1982).
[31]Y. Fujita, M. Fujiwara, S. Morinobu, T. Yamazaki, T. Itahashi, S. Imanishi, K. Ikegami, and S. I. Hayakawa, Phys. Rev. C **25**, 678 (1982).
[32]G. R. Satchler, Nucl. Phys. **A195**, 1 (1972).
[33]L. G. Multhauf, K. G. Tirsell, S. Raman, and J. B. McGrory, Phys. Lett. **57B**, 44 (1975).
[34]M. Fujiwara, Y. Fujita, S. Imanishi, S. Morinobu, T. Yamazaki, H. Ikegami, K. Katori, and S. I. Hayakawa, Phys. Rev. C **32**, 830 (1985).
[35]B. D. Anderson, J. N. Knudson, P. C. Tandy, J. W. Watson, R. Madey, and C. C. Foster, Phys. Rev. Lett. **45**, 699 (1980).
[36]W. Steffen, H.-D. Gräf, W. Gross, D. Meuer, A. Richter, E. Spamer, O. Titze, and W. Knupfer, Phys. Lett **95B**, 23 (1980).
[37]G. P. A. Berg, W. Hurlimann, I. Katayama, S. A. Martin, J. Meissburger, J. Romer, B. Styczen, F. Osterfeld, G. Gaul, R. Santo, and G. Sonderman, Phys. Rev. C **25**, 2100 (1982).
[38]G. M. Crawley, N. Anantaraman, A. Galonsky, C. Djalali, N. Marty, M. Morlet, A. Willis, and J. C. Jourdain, Phys. Lett. **127B**, 322 (1983).
[39]C. Djalali, N. Marty, M. Morlet, A. Willis, J. C. Jourdain, N. Anantaraman, G. M. Crawley, A. Galonsky, and J. Duffy, Nucl. Phys. **A410**, 399 (1983).
[40]H. V. von Geramb, L. Rikus, and N. Nakano, in Proceedings of the 1983 Research Center for Nuclear Physics International Symposium on Light Ion Reaction Mechanism, Osaka, p. 78; and H. V. von Geramb, private communication.
[41]G. Bertsch, J. Borysowicz, H. McManus, and W. G. Love, Nucl. Phys. **A284**, 399 (1977).
[42]W. Steffen, H.-D. Gräf, A. Richter, A. Härting, W. Weise, U. Deutschmann, G. Lahum, and R. Neuhausen, Nucl. Phys. **A404**, 413 (1983).
[43]F. E. Bertrand, Nucl. Phys. **A354**, 129 (1981), and references therein.
[44]D. H. Youngblood, P. Bogucki, J. D. Bronson, U. Garg, Y.-W. Lui, and C. M. Rosza, Phys. Rev. C **23**, 1997 (1981).
[45]Y.-W. Lui, J. D. Bronson, D. H. Youngblood, Y. Toba, and U. Garg, Phys. Rev. C **31**, 1643 (1985).
[46]H. J. Lu, S. Brandenburg, R. De Leo, M. N. Harakeh, T. D. Poelhekken, and A. van der Woude, Phys. Rev. C **33**, 1116 (1986).
[47]S. Brandenburg, R. De Leo, A. G. Drentje, M. N. Harakeh, H. Sakai, and A. van der Woude, Phys. Lett. **130B**, 9 (1983).
[48]R. J. Peterson, Phys. Rev. Lett. **57**, 1550 (1986).
[49]J. Blomquist and A. Molinari, Nucl. Phys. **A106**, 545 (1968).
[50]C. Mayer-Böricke, W. Oelert, A. Kiss, M. Rogge, P. Turek, and S. Wiktor, Nucl. Phys. **A293**, 189 (1977).
[51]J. M. Moss, D. R. Brown, D. H. Youngblood, C. M. Rozsa, and J. D. Bronson, Phys. Rev. C **18**, 741 (1978).
[52]J. Speth and A. van der Woude, Rep. Prog. Phys. **44**, 719 (1981), and references therein.
[53]G. F. Bertsch, P. F. Bortignon, and R. A. Broglia, Rev. Mod. Phys. **55**, 287 (1983).
[54]Y. Fujita, M. Fujiwara, S. Morinobu, I. Katayama, T. Yamazaki, T. Itahashi, H. Ikegami, and S. I. Hayakawa, Phys. Lett. **98B**, 175 (1981).
[55]K. Arita, private communication.